A kinesin-13 mutant catalytically depolymerizes microtubules in ADP

Michael Wagenbach,[1,2] Sarah Domnitz,[1] Linda Wordeman,[1,2] and Jeremy Cooper[1]

[1]Deptartment of Physiology and Biophysics, University of Washington School of Medicine, Seattle, WA 98107
[2]Center for Cell Dynamics, Friday Harbor Laboratories, Friday Harbor, WA 98250

The kinesin-13 motor protein family members drive the removal of tubulin from microtubules (MTs) to promote MT turnover. A point mutation of the kinesin-13 family member mitotic centromere-associated kinesin/Kif2C (E491A) isolates the tubulin-removal conformation of the motor, and appears distinct from all previously described kinesin-13 conformations derived from nucleotide analogues. The E491A mutant removes tubulin dimers from stabilized MTs stoichiometrically in adenosine triphosphate (ATP) but is unable to efficiently release from detached tubulin dimers to recycle catalytically. Only in adenosine diphosphate (ADP) can the mutant catalytically remove tubulin dimers from stabilized MTs because the affinity of the mutant for detached tubulin dimers in ADP is low relative to lattice-bound tubulin. Thus, the motor can regenerate for further cycles of disassembly. Using the mutant, we show that release of tubulin by kinesin-13 motors occurs at the transition state for ATP hydrolysis, which illustrates a significant divergence in their coupling to ATP turnover relative to motile kinesins.

Introduction

Microtubules (MTs) spontaneously change length by the assembly and disassembly of tubulin dimers (Mitchison and Kirschner, 1984), and members of the kinesin-13 family promote MT turnover or dynamics by driving the removal of tubulin from MTs (Hunter et al., 2003). Highly dynamic MTs are a hallmark of both rapidly dividing and metastatic cells (Jordan and Wilson, 1998; Goncalves et al., 2001). The kinesin-13 family member mitotic centromere-associated kinesin (MCAK) is the most potent MT-depolymerizing ATPase so far identified, and is often up-regulated during tumorigenesis (Nakamura et al., 2007; Shimo et al., 2008). Yet, the role of ATP turnover in the disassembly of MTs by MCAK remains unclear (Ogawa et al., 2004). Previous structural studies have proposed that ATP hydrolysis is coupled to tubulin protofilament bending, and that tubulin release from MCAK would be coupled to phosphate release (Desai et al., 1999; Ogawa et al., 2004; Shipley et al., 2004; Helenius et al., 2006). Instead, using mutational analysis, we define a reaction scheme for MCAK that is related to that of motile kinesins but is distinct in the relationship between the nucleotide states and reaction coordinates.

Kinesin and myosin superfamily motor proteins use conserved structural elements to effect ATP hydrolysis and respond to different nucleotide states (Sablin et al., 1996). Residues in the regions named Switch I (consensus sequence: NxxSSR) and Switch II (DxxGxE) form a network of hydrogen bonds with the nucleotide, Mg^{2+}, and each other. This network senses the presence or absence of the γ-phosphate and triggers both ATP hydrolysis and allosteric changes in the motor structure (Naber et al., 2003; Nitta et al., 2004; Hirose et al., 2006). Switch II is directly connected to the MT-binding site in the kinesin superfamily (Woehlke et al., 1997; Kikkawa et al., 2001). Recent cryoelectron microscopic studies suggest that alterations in these structures and in their contacts with tubulin among different nucleotide states (ADP, no nucleotide, and adenylyl-imidodiphosphate [AMPPNP]) may explain the changes in MT affinity between different nucleotide states (Hirose et al., 2006).

The structural and enzymatic effects of mutating the conserved G and E residues of Switch II to alanine have been well characterized for myosin motors (Sasaki et al., 1998). The G-to-A mutant is presumed to conform to a pre-ATP–like state that precedes the recovery stroke of the myosin head, whereas the E-to-A mutant is interpreted to correspond to a transition state leading to ATP hydrolysis, which allows the recovery stroke (Suzuki et al., 1998). In kinesin-1, the corresponding mutations

Correspondence to Linda Wordeman: worde@u.washington.edu

Abbreviations used in this paper: AMPPNP, adenylyl-imidodiphosphate; MCAK, mitotic centromere-associated kinesin; MT, microtubule; TIRF, total internal reflection fluorescence; wt, wild type.

The online version of this article contains supplemental material.

The Rockefeller University Press $30.00
J. Cell Biol. Vol. 183 No. 4 617–623
www.jcb.org/cgi/doi/10.1083/jcb.200805145

also appear to correspond to analogous states before and after the docking of the neck linker to the MT-bound motor head. Neck linker docking allows the unbound head to move to its next binding site toward the plus end of the MT. This docking is also promoted by AMPPNP, so in kinesin-1 as well, the E-to-A mutant appears to occupy a point on the ATP cycle that immediately precedes or accompanies ATP hydrolysis (Rice et al., 1999; Tomishige et al., 2006). Mutations in the Switch II domain drastically reduce ATP turnover by blocking the hydrolysis step. A detailed reaction scheme linking steps in the ATP hydrolysis cycle and motility for kinesin-1 has been described recently (Guydosh and Block, 2006).

Biochemical and microscopic analysis of a point mutant in the Switch II region of MCAK (E491A) establishes that binding and detachment of tubulin from the MT occurs before ATP hydrolysis. This model is confirmed by our observation that in the presence of ADP, E491A is capable of detaching tubulin dimers from stabilized MTs and then recycling back onto the lattice to release 18 moles of tubulin per mole of motor. This slow catalysis contrasts with the behavior of the E491A in ATP, in which the mutant is capable of detaching a tubulin dimer, but only on a mole-per-mole basis. The mutant, presumably because of its unique conformation, remains strongly bound to the detached tubulin dimer and is unable to recycle back onto lattice. Thus, in the high-ATP environment of living cells, exogenously expressed E491A disassembles MTs via tubulin sequestration without triggering the tubulin autoregulatory response. We have previously demonstrated that disassembly of MTs in living cells via overexpression of wild-type (wt) MCAK leads to dose-dependent inhibition of endogenous cellular tubulin expression (Ovechkina et al., 2002). In summary, our data demonstrate that tubulin detachment by wt MCAK is completed before ATP hydrolysis and is mimicked by the E491A mutant. Release of detached tubulin dimer by the motor is correlated with the attainment of the transition state for ATP hydrolysis. Thus, in wt MCAK, detachment of tubulin may trigger ATP hydrolysis. This feature differs from other kinesins in which the motor remains strongly bound to lattice during the attainment of the transition state for ATP hydrolysis (Asenjo et al., 2006). We speculate that the kinesin-13 family may represent an early branch in the evolution of kinesin subfamilies.

Results and discussion

We engineered two mutants that correspond to the conserved G and E residues of Switch II (G489A and E491A; Fig. S1, available at http://www.jcb.org/cgi/content/full/jcb.200805145/DC1). When we assayed them in our in vivo depolymerization assay (Ovechkina et al., 2002), we found that total tubulin levels remained high even in cells with few or no visible MTs (Fig. 1). This contrasts with wt MCAK overexpression, which increases free tubulin dimers and triggers autoregulated tubulin translational suppression that is measurable as a dose-dependent decrease in total tubulin fluorescence (Ovechkina et al., 2002). In contrast, tubulin released by E491 (and to a lesser extent G489A) does not trigger translational repression of tubulin. We hypothesized that these mutant proteins remained bound to tubulin after

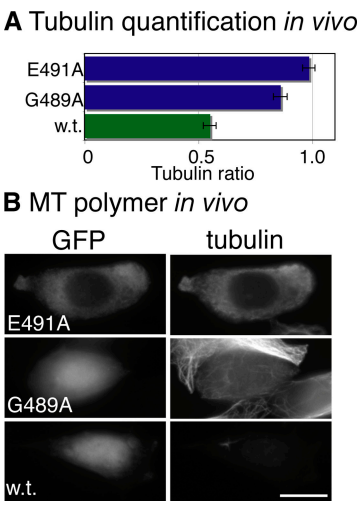

Figure 1. **Switch II mutants sequester tubulin in vivo.** (A) Cells transfected with E491A or G489A mutant MCAK have near-normal total tubulin content. For E491A and G489A, n = 52 cells; for wt, n = 38 cells. Error bars indicate SEM of the tubulin ratio. (B) Images of representative cells containing wt EGFP-MCAK, G489A mutant (G), or E491A mutant (E). Although quantification shows near normal tubulin content, immunofluorescence reveals that most of the MT polymer is gone, which suggests that the MTs have been disassembled via tubulin sequestration. Bar, 10 µm.

removing it from MTs, and sequestered it from normal tubulin translational regulation (Cleveland et al., 1981). This suggested that the Switch II mutants are impaired in the final step of catalytic MT disassembly: the release of the detached tubulin dimer.

Consistent with this hypothesis, purified full-length E491A bound tubulin in vitro in ATP with much higher affinity (K_d = 230 nM) than wt MCAK (K_d = 4.7 µM; Fig. 2). We found that E491A exhibited lower tubulin affinity in ADP-Al-F, an ATP hydrolysis transition state analogue (Fisher et al., 1995; Nitta et al., 2004), which indicates that tubulin release occurs in concert with ATP hydrolysis, not P_i release, as has been previously suggested (Hunter et al., 2003). Although the E491A mutant has a very low basal ATPase rate, the ATPase is still sensitive to stimulation by MTs or unpolymerized tubulin (Fig. S2, available at http://www.jcb.org/cgi/content/full/jcb.200805145/DC1). The $K_{1/2,tubulin}$ (the tubulin concentration at which the ATPase rate is half-maximal, analogous to the K_d for tubulin) for E491A is 39 nM tubulin, whereas the $K_{1/2,tubulin}$ for wt MCAK is 1.5 µM, which confirms that the mutant has a much tighter association with tubulin.

Surprisingly, purified recombinant E491A MCAK was able to depolymerize MTs in vitro in the presence of either ATP or ADP (Figs. 3 and S3 A, available at http://www.jcb.org/cgi/content/full/jcb.200805145/DC1). wt EGFP-MCAK depolymerized MTs catalytically in ATP, releasing ~0.05 tubulin dimers per MCAK per second (Fig. 3, A and B). Neither ADP nor the nucleotide analogues AMPPNP or ADP-Al-F were able to promote depolymerization by wt MCAK, even at a stoichiometry of 1:3 MCAK/tubulin (Fig. 3 B), which indicates that completion of the normal nucleotide hydrolysis cycle is required for depolymerization. In contrast, E491A released somewhat more tubulin in ADP or ADP-Al-F than in ATP, though at an apparent rate that was lower than for wt MCAK, releasing 0.002–0.003 dimers per MCAK per second. The pre-ATP state mimic G489A

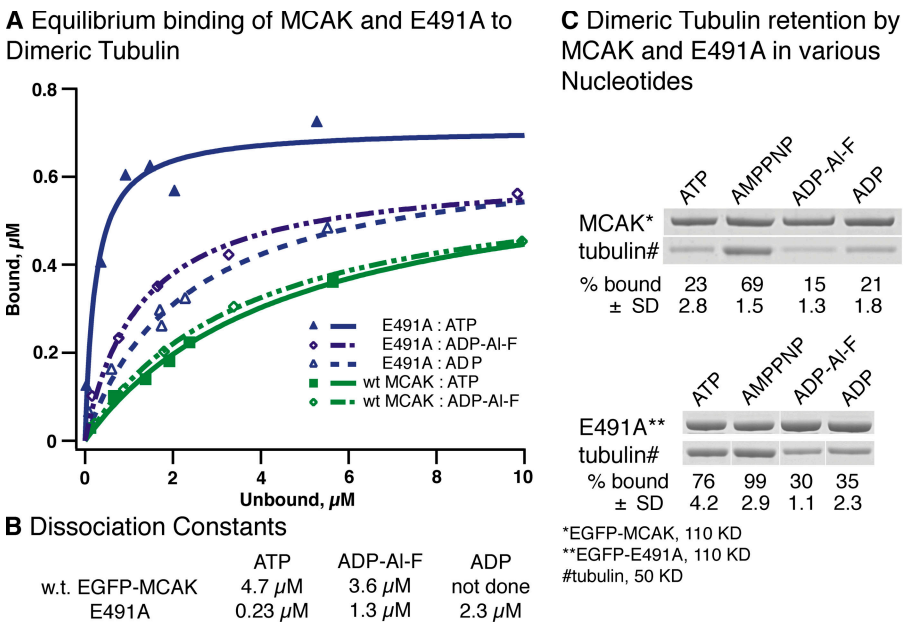

Figure 2. **The effect of various nucleotides and E491A mutation on equilibrium binding of MCAK to tubulin dimers.** (A) Tubulin-binding assays with 700 nM MCAK, 150 μM of indicated nucleotide, and bound versus unbound bovine brain tubulin. (B) Dissociation constants (K_d) from fit curves. (C) Comparison of tubulin retention by wt MCAK and E491A in various nucleotides (1.6 mM) and a constant concentration of tubulin (2 μM). The percentage of tubulin dimer bound to the motor in each nucleotide and standard deviation from the mean (SD) are indicated. All lanes, respectively, are run on the same gel but the order of the lanes in E491A (bottom) are arranged to correspond to the nucleotide order of wt MCAK (top).

failed to promote any depolymerization in vitro in ATP-containing buffer (unpublished data), and was not analyzed further. The rate of depolymerization by E491A in ATP appeared to decline as free tubulin reached a concentration approximately equal to that of the mutant MCAK (Fig. 3 B, broken line), which suggests a product-inhibition effect mediated by tighter binding to tubulin in ATP than in ADP.

We directly observed E491A-MCAK depolymerizing MTs in a reaction mix containing excess MTs with a total internal reflection fluorescence (TIRF) microscope (Fig. 3 C, Fig. S3 B, and Video 1, available at http://www.jcb.org/cgi/content/full/jcb.200805145/DC1). The assay was performed at different motor concentrations designed to mimic the following stoichiometries: 1:3 (the stoichiometry for E491A in Fig. 3 B), 1:1.7, and supersaturated (1.3:1) stoichiometry, in which all tubulin dimers are expected to be complexed with E491A. Linear depolymerization rates were measured during the first 60–180 s of depolymerization at three E491A concentrations while holding the tubulin (MT) concentration constant. The TIRF rate of depolymerization in ADP (Fig. 3 C, 0.007 dimers motor^{-1}s^{-1}) correlated well with the data obtained from the pelleting assays (Fig. 3 B, 0.002 dimers motor^{-1}s^{-1}). As expected, the rate of depolymerization by E491A was significantly decreased ($P < 0.001$) in the presence of ATP under the same conditions. It is important to note that the rate of MT disassembly by wt kinesin-13 motors changes depending on the ratio of motor to tubulin. Previously, it has been shown that the rate of wt MCAK disassembly is maximal when the MT end-binding sites are saturated (10–13 motors per MT end; approximately one per protofilament; Hunter et al., 2003). E491A is distinctly different from wt MCAK in that its rate of MT disassembly continues to increase until all the tubulin-binding sites, not just the protofilament end sites, are saturated (Fig. 3 C, dark blue). In contrast, the reaction rate in ADP is virtually constant in the range of motor concentrations tested, even though the concentration of E491A on the MT does increase (Fig. S3 B), which indicates that the rate-limiting step in ADP occurs after arrival of the enzyme at the protofilament end. At a high enzyme concentration, in which the effect of tubulin binding and sequestration of the motor is insignificant, the rate in ATP is faster than in ADP (Fig. 3 C). These results can be understood based on a model in which ATP–MCAK induces or stabilizes a curved configuration of tubulin at the protofilament end (Desai et al., 1999; Moores et al., 2002; Shipley et al., 2004; Elie-Caille et al., 2007). By extension from our observation of E491A's lower affinity for the curved free tubulin dimer, we expect that E491A–ADP has a lower affinity than E491A–ATP for the curved configuration of the tubulin in the protofilament end required to cause depolymerization. Thus, by analogy to the hare and the tortoise, E491A in ATP is very effective at removing tubulin dimers but cannot recycle itself; E491 in ADP is less efficient at removing tubulin dimers but can recycle to accomplish further rounds of tubulin removal (diagrammed in Fig. 4, A–C).

To verify that E491A depolymerization is catalytic in ADP, we monitored the turbidity of reactions in which MCAK was approximately equimolar with protofilament ends (Fig. 3 D). In the turbidity experiments, the stoichiometry was 1:117 motor/tubulin or 1.4 motors per protofilament end for both wt MCAK and E491A. At this stoichiometry, no depolymerization could be detected by E491A–ATP, although we cannot be sure there is no activity because removal of one equivalent or a small molar excess of tubulin would give too small a change in turbidity to detect reliably. In contrast, after subtraction of background from control reactions, ~18 moles of tubulin were released per mole of E491A in ADP over the course of the experiment, which indicates robust catalysis. At this stoichiometry, wt MCAK, a proven catalytic MT depolymerizer, released ~28 moles of tubulin per mole of motor. Because E491A's catalytic depolymerization occurs in the absence of ATP, we conclude that the energy source for MCAK's depolymerization activity is the binding energy between MCAK and tubulin, and that ATP hydrolysis gates tubulin release in wt MCAK. This tubulin release step is inhibited by ATP in the E491A mutant.

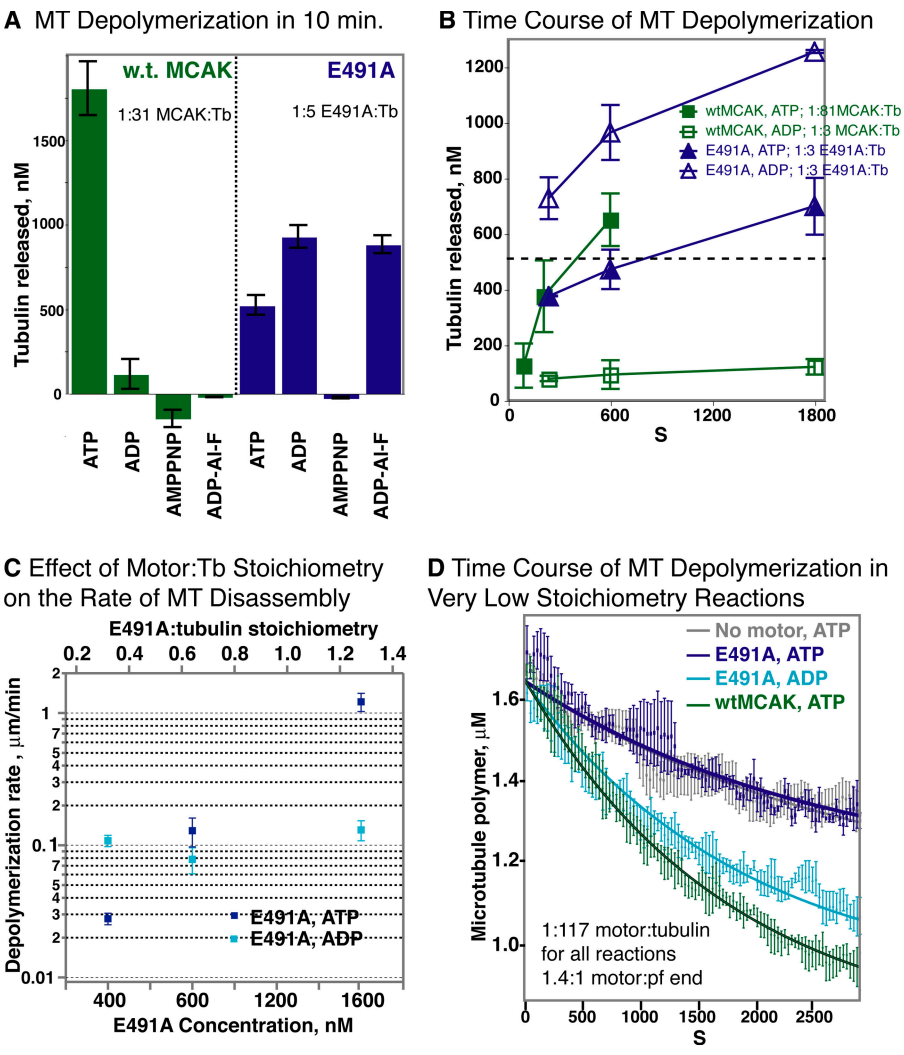

Figure 3. **In vitro depolymerization in various nucleotide states and MCAK–tubulin stoichiometries.** (A) MT depolymerization reactions performed for 10 min at 23°C with 0.5 mM of the indicated nucleotide and 2.5 μM GMPCPP-tubulin MTs, stopped by centrifugation. Enzyme concentration: 80 nM wt MCAK in ATP (1:31 MCAK/tubulin) and 510 nM in all other reactions (1:5). Tubulin release was measured by a pelleting assay using the stoichiometries of active motor to total tubulin indicated. Values are normalized to control (no motor) tubulin release of 0.13 nM per second (SD 0.02 nM). In contrast to wt MCAK, E491A releases more tubulin in ADP and ADP-Al-F than in ATP. (B) Time course of depolymerization as in A, except 1.7 μM GMPCPP tubulin, 21 nM wt MCAK in ATP (1:81 motor/tubulin), and 510 nM in all other reactions (1:3 motor/tubulin). E491A (at 510 nM) releases 1,200 nM tubulin dimers in 30 min in ADP, which suggests that the motor is recycling. In contrast, in ATP, less than equimolar tubulin is released in 30 min by E491A. (C) Linear depolymerization rates of MT ends directly observed in TIRF microscope. MTs tethered to a coverslip observed in a reaction chamber containing 1.25 μM of GMPCPP-Cy5-tubulin MTs, 2 mM of the indicated nucleotide, and 400–1,600 nM EGFP-E491A-MCAK. The rates are normalized to the nonmotor control tubulin loss rates that were observed to be 0.08 nM per second (SD, 0.03). E491A is capable of disassembling MTs at a high rate in ATP but only when the proportion of motor exceeds that of tubulin. At ∼1:3 motor/tubulin, E491A depolymerizes MTs at a higher rate in ADP than in ATP. (D) Loss of MT polymer observed by light scattering at very low stoichiometry (1:117 motor/tubulin or 1.4:1 MCAK/protofilament ends). Turbidity of reaction mixes with 0.2 mM of the indicated nucleotide, 14 nM MCAK, and 1.64 μM GMPCPP tubulin as 2.5-μm mean length MTs (10.6 nM protofilament ends) at 23°C and monitored at 340 nm. The rate of tubulin loss in the absence of motor and free tubulin is 0.10 nM per second (SD, 0.02), which is consistent with the control rates of tubulin loss for the pelleting and TIRF assays. At <1:100 motor per tubulin stoichiometry, E491A is incapable of disassembling MTs in ATP, whereas in ADP, ∼18 moles of tubulin were released per mole of E491A, indicating that the motor is recycling during successive rounds of tubulin removal. pf, protofilament. Error bars indicate SD of the measured quantity (tubulin released or the linear depolymerization rate).

Significantly, AMPPNP blocked depolymerization by the mutant protein (Fig. 3 A), thus the AMPPNP-bound state and the E491A state in other nucleotides are not equivalent and represent two successive states within the hydrolysis cycle of MCAK (diagrammed in Fig. 4 D). Kinesin-1 in AMPPNP allows docking of the neck linker to the head domain, though transiently, compared with the more tightly docked ADP-Al-F state (Asenjo et al., 2006), which indicates that the AMPPNP state is early in the reaction scheme. We speculate that for MCAK, AMPPNP stabilizes the predepolymerization configuration even in the E491A mutant, but that ADP or ADP-Al-F enables the mutant to reach a configuration that is farther along the depolymerization reaction coordinate than the AMPPNP state (Fig. 4 D). wt MCAK is known to bind and accumulate at MT ends in AMPPNP, causing shortening of the MTs by fraying of the lattice into protofilament curls, but this does not result in tubulin detachment from the lattice (Desai et al., 1999). A monomeric deletion construct in AMPPNP also frays MTs into oligomeric protofilaments (Moores et al., 2006), which indicates that the effect seen in AMPPNP is not caused by cross-linking of depolymerized tubulin by dimeric MCAK. We conclude that full depolymerization requires the attainment of the transition state for ATP hydrolysis that lies beyond the AMPPNP state. Attainment of this state either forces the tubulin dimer off the protofilament end or alters its affinity with neighboring tubulin. Because monomeric deletion constructs can promote full depolymerization in ATP (Maney et al., 2001), we favor the latter mechanism through an allosteric effect between MCAK and tubulin, as the forceful separation of the tubulin dimers would seem to require dimeric MCAK, with its two tubulin binding sites.

Neither E491A nor wt MCAK bind tubulin dimers with high affinity in ADP-Al-F (Fig. 2), which shows that this state and tubulin release occur later in the cycle and are distinct from the depolymerization step. ADP-Al-F has been seen to form a bipyramidal transition state in crystal structures of both myosin and kinesin Kif1A, so ADP-Al-F is expected to represent a transition state, not, as sometimes reported, the ADP-Pi state, of MCAK. We conclude that MCAK has two transition states along

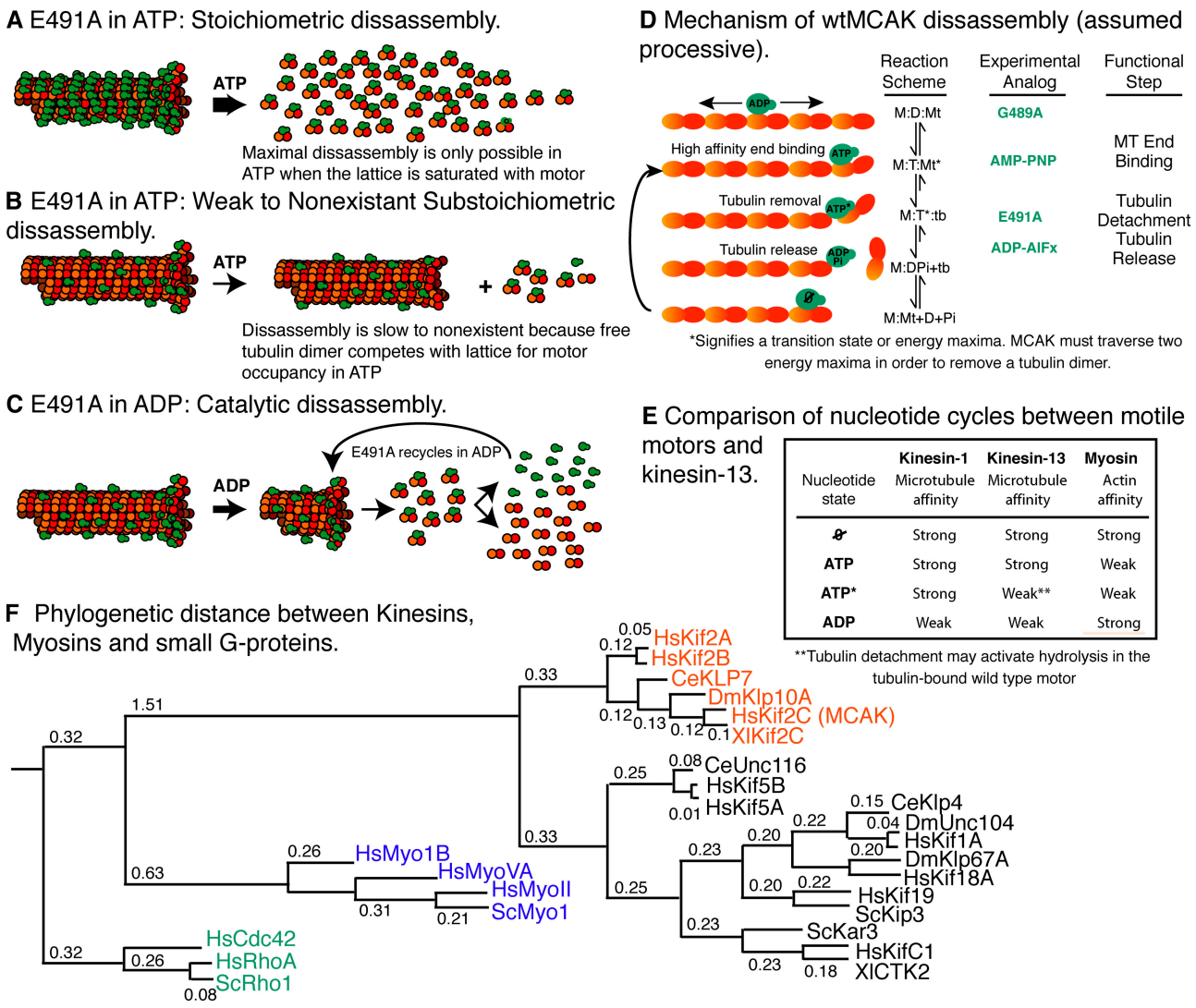

Figure 4. **A model of the MCAK depolymerization reaction.** (A) MTs supersaturated with E491A can be rapidly disassembled in ATP. (B) The lower the ratio of E491A to tubulin, the less effective the motor is in disassembling MTs in ATP. (C) E491A is capable of steady catalytic disassembly of MTs in ADP because the motor can release from tubulin and recycle back onto MT lattice. (D) A model for MCAK-dependent disassembly of MTs. Our data suggests that MCAK can completely remove one tubulin dimer before ATP hydrolysis. M:D:Mt represents ADP–MCAK diffusing on MT, M:T:Mt* represents the first ATP–MCAK depolymerization transition state, M:T*:tb represents the ATP hydrolysis transition state/low tubulin affinity transition state, and M:DPi + tb represents ADP-Pi–MCAK dissociated from tubulin dimer. A postulated zero ATP state is also shown. This state exhibits high affinity for the MT lattice (Moore and Wordeman, 2004). (E) MCAK's affinity for tubulin decreases upon reaching the ATP transition state, unlike motile kinesins. (F) Phylogenetic distances based on an alignment of the Switch I, Switch II, and the P-loop of kinesins, myosins, and G proteins. Alignments are shown in Fig. S4 (available at http://www.jcb.org/cgi/content/full/jcb.200805145/DC1).

its reaction coordinate, the first for tubulin detachment from the MT and the second for tubulin release from MCAK, and that the E491A mutant occupies a state that is intermediate between the AMPPNP and ADP-Al-F states (Fig. 4 D).

Although kinesin-1's forward step can occur in AMPPNP, MCAK cannot remove a tubulin dimer in the presence of this analogue, which mimics the ATP collision state. Instead, MCAK's tubulin detachment step occurs before the transition state represented by ADP-Al-F. Attainment of this transition state reduces the affinity of MCAK for the detached tubulin dimer, promoting the release of dimer from the motor (Fig. 4, D and E). Thus, the entire process of tubulin removal from the MT occurs before ATP hydrolysis. In contrast, kinesin-1 has a high MT affinity in ADP-Al-F (Asenjo et al., 2006), and unbinding is coupled with ADP or P_i release (Schief et al., 2004; Guydosh and Block, 2006). It is tempting to speculate that detachment of the tubulin dimer from MT lattice may, in fact, promote ATP hydrolysis. This may be the explanation for the increased catalytic efficiency of wt MCAK over E491A, which behaves more like a conventional catalyst that does not actively alter itself to participate in a reaction.

Although kinesin-13 and kinesin-1 share highly homologous motor domains, their very different interactions with MTs are accompanied by remarkable divergence in their coupling to the ATPase reaction cycle. To gain some insight into this evolutionary divergence, we compared the phylogenetic distance between the Switch I, Switch II, and P-loop domains of myosins, kinesins, and ancestral G proteins (Fig. 4 F). We hypothesize that the kinesin-13 family may have diverged relatively early in the evolution of the kinesin subfamilies.

Materials and methods

In vivo depolymerization assay
MCAK activity was quantified in vivo as described previously (Ovechkina et al., 2002). In brief, EGFP-MCAK–transfected cells were fixed and stained with anti-tubulin antibody. Cells were selected such that the EGFP level was equivalent to the amount of wt EGFP-MCAK observed to be just sufficient to depolymerize essentially all MTs in the cell. Tubulin-staining ratios between transfected cells and untransfected cells in the same field were calculated ("tubulin ratio"). wt MCAK-transfected cells with fully depolymerized MTs have a tubulin ratio of ~0.5, whereas cells transfected with GFP alone have an MT ratio of 1. Mutant EGFP-MCAK is expected to give a tubulin ratio greater than in wt cells if depolymerization is impaired.

Protein purification
We purified mutant full-length EGPF-MCAK-6H proteins for in vitro studies from a baculovirus expression system as described previously (Maney et al., 1998), except that the pFastBac1 plasmid (Invitrogen) was used to construct recombinant baculoviruses. All MCAK concentrations are described as active sites, although the protein is believed to be dimeric (Maney et al., 1998).

Tubulin-binding assay
Recombinant EGFP-MCAK was incubated in buffer containing 1.6 mM of the indicated nucleotide for 3.5 h on ice, then incubated at 700 nM MCAK in BRB80 + 75 mM KCl + 150 µM of the indicated nucleotide with 0.15–10 µM bovine brain tubulin and Ni-NTA–agarose beads (QIAGEN) for 45 min at 23°C, transferred to spun columns, and washed once in 0.5 ml of the same buffer. Bound proteins were eluted with 500 mM imidazole-HCl and run on SDS-NuPAGE gels (Invitrogen). Coomassie-stained gels were dried, scanned, and measured using ImageJ, and the bound versus free tubulin was fit by nonlinear regression to calculate K_d using IgorPro (WaveMetrics).

In vitro depolymerization pelleting assay
Stabilized MTs were prepared from bovine brain tubulin by two cycles of polymerization and pelleting from GMPCPP solution. The final cycle was pelleted through a cushion of 20% glycerol in BRB80 to remove free GMPCPP, and resuspended in BRB80 + 1 mM DTT + 0.2 mg/ml BSA. MT depolymerization assays were performed in BRB80 + 75 mM KCl + 1 mM DTT + 0.2 mg/ml BSA + 0.5 mM GDP + 0.2 mM ATP with 2.5 µM tubulin at 23°C before centrifugation in an ultracentrifuge (Airfuge; Beckman Coulter) for 10 min at 30 psi. Equal fractions of supernatant and pellet samples were run on SDS-NuPAGE gels (Invitrogen) and stained with Coomassie R-250. Depolymerization was corrected for unpelleted tubulin in buffer blank control reactions. For assays in nucleotides other than ATP, 4× concentrated MCAK solution was incubated in 2.5 mM AMPPNP, ADP, or ADP-Al-F for 3 h on ice before dilution into reaction buffer.

TIRF microscopy depolymerization assay
TIRF data were collected using an inverted microscope (TE2000-S; Nikon) with a custom-built two-color TIRF illumination system. GFP was excited with a 473-nm laser (LaserPath Technologies), and Cy5 was excited with a 637-nm laser (Blue Sky Research). Red and green images were split with a dichroic mirror and projected side by side onto the camera charge-coupled device (CCD) to allow full simultaneous two-color imaging. Images were recorded at one frame per second on a back-illuminated EMCCD (Ixon DV887ECS-BV; Andor). Nonspecific protein adsorption was virtually eliminated by coating coverslips with a short-chain polyethylene glycol–silane (Gelest, Inc.) and blocking with κ-casein (Sigma-Aldrich). Cy5-labeled, GMPCPP-stabilized MTs were tethered to the coverslip surface by a rigor-kinesin Kif5b, courtesy of the Vale Laboratory. EGFP-MCAK was mixed with additional GMPCPP-stabilized MTs at the noted concentrations, then immediately pumped into the viewing chamber. The pump was then set at a slow speed during the entirety of the data collection period to prevent the MTs in solution from interacting with the MTs tethered to the surface. In this way, the concentrations of both MCAK and MTs in solution could be controlled while still allowing MTs at the coverslip surface and the EGFP-MCAK bound to them to be accurately imaged. MT ends were precisely located using an edge-finding routine in Igor. Two to three separate flow cells were prepared per experimental condition (10 or more MTs per flow cell were analyzed). From this data, the MT lengths and corresponding rates of shortening were calculated. Mean lattice brightness in the green channel was also calculated using Igor.

In vitro depolymerization turbidity assay
MTs cycled twice in GMPCPP were diluted to 1.64 µM in buffer as for the pelleting assay, except with 14 nM MCAK and 100 µM ADP or ATP. The turbidity was measured every 6 s in a 1-cm path-length cuvette at 340 nm. After 3,000 s, 10 mM $CaCl_2$ was added to depolymerize remaining MTs and establish a baseline reading. Loss of MT polymer (Y) was fit to a one-phase exponential decay $Y = (Y_0)^{(-KX)}$ using GraphPad Prism (GraphPad Software). In this case, Y_0 = initial tubulin polymer concentration of 1.6 M (K = rate constant and X = time). Each experimental condition was performed identically 3–5 times on different days and averaged to obtain the error.

Online supplemental material
Fig. S1 shows a space-filling model showing the position of key residues in Switch I and Switch II. Fig. S2 shows tubulin-stimulated and MT-stimulated ATPase of recombinant EGFP-MCAK and E491A mutant. Fig. S3 shows in vitro depolymerization in various nucleotide states and MCAK–tubulin stoichiometries. Table S1 shows alignments used to build the distance tree in Fig. 4 F. Video 1 shows TIRF microscopy of MTs depolymerizing in the presence of two different E491 stoichiometries. Online supplemental material is available at http://www.jcb.org/cgi/content/full/jcb.200805145/DC1.

We thank members of the Asbury, Davis, and Wordeman laboratories for comments on the manuscript.

This work was supported by National Institutes of Health grants to L. Wordeman (GM69429) and S. Domnitz (GM007270).

Submitted: 26 May 2008
Accepted: 6 October 2008

References

Asenjo, A.B., Y. Weinberg, and H. Sosa. 2006. Nucleotide binding and hydrolysis induces a disorder-order transition in the kinesin neck-linker region. *Nat. Struct. Mol. Biol.* 13:648–654.

Cleveland, D.W., M.A. Lopata, P. Sherline, and M.W. Kirschner. 1981. Unpolymerized tubulin modulates the level of tubulin mRNAs. *Cell.* 25:537–546.

Desai, A., S. Verma, T.J. Mitchison, and C.E. Walczak. 1999. Kin I kinesins are microtubule-destabilizing enzymes. *Cell.* 96:69–78.

Elie-Caille, C., F. Severin, J. Helenius, J. Howard, D.J. Muller, and A.A. Hyman. 2007. Straight GDP-tubulin protofilaments form in the presence of taxol. *Curr. Biol.* 17:1765–1770.

Fisher, A.J., C.A. Smith, J. Thoden, R. Smith, K. Sutoh, H.M. Holden, and I. Rayment. 1995. Structural studies of myosin:nucleotide complexes: a revised model for the molecular basis of muscle contraction. *Biophys. J.* 68:19S–28S.

Goncalves, A., D. Braguer, K. Kamath, L. Martello, C. Briand, S. Horwitz, L. Wilson, and M.A. Jordan. 2001. Resistance to Taxol in lung cancer cells associated with increased microtubule dynamics. *Proc. Natl. Acad. Sci. USA.* 98:11737–11742.

Guydosh, N.R., and S.M. Block. 2006. Backsteps induced by nucleotide analogs suggest the front head of kinesin is gated by strain. *Proc. Natl. Acad. Sci. USA.* 103:8054–8059.

Helenius, J., G. Brouhard, Y. Kalaidzidis, S. Diez, and J. Howard. 2006. The depolymerizing kinesin MCAK uses lattice diffusion to rapidly target microtubule ends. *Nature.* 441:115–119.

Hirose, K., E. Akimaru, T. Akiba, S.A. Endow, and L.A. Amos. 2006. Large conformational changes in a kinesin motor catalyzed by interaction with microtubules. *Mol. Cell.* 23:913–923.

Hunter, A.W., M. Caplow, D.L. Coy, W.O. Hancock, S. Diez, L. Wordeman, and J. Howard. 2003. The kinesin-related protein MCAK is a microtubule depolymerase that forms an ATP-hydrolyzing complex at microtubule ends. *Mol. Cell.* 11:445–457.

Jordan, M.A., and L. Wilson. 1998. Microtubules and actin filaments: dynamic targets for cancer chemotherapy. *Curr. Opin. Cell Biol.* 10:123–130.

Kikkawa, M., E.P. Sablin, Y. Okada, H. Yajima, R.J. Fletterick, and N. Hirokawa. 2001. Switch-based mechanism of kinesin motors. *Nature.* 411:439–445.

Maney, T., A.W. Hunter, M. Wagenbach, and L. Wordeman. 1998. Mitotic centromere-associated kinesin is important for anaphase chromosome segregation. *J. Cell Biol.* 142:787–801.

Maney, T., M. Wagenbach, and L. Wordeman. 2001. Molecular dissection of the microtubule depolymerizing activity of mitotic centromere-associated kinesin. *J. Biol. Chem.* 276:34753–34758.

Mitchison, T., and M. Kirschner. 1984. Dynamic instability of microtubule growth. *Nature.* 312:237–242.

Moore, A., and L. Wordeman. 2004. C-terminus of mitotic centromere-associated kinesin (MCAK) inhibits its lattice-stimulated ATPase activity. *Biochem. J.* 383:227–235.

Moores, C.A., M. Yu, J. Guo, C. Beraud, R. Sakowicz, and R.A. Milligan. 2002. A mechanism for microtubule depolymerization by KinI kinesins. *Mol. Cell.* 9:903–909.

Moores, C.A., J. Cooper, M. Wagenbach, Y. Ovechkina, L. Wordeman, and R.A. Milligan. 2006. The role of the kinesin-13 neck in microtubule depolymerization. *Cell Cycle.* 5:1812–1815.

Naber, N., T.J. Minehardt, S. Rice, X. Chen, J. Grammer, M. Matuska, R.D. Vale, P.A. Kollman, R. Car, R.G. Yount, et al. 2003. Closing of the nucleotide pocket of kinesin-family motors upon binding to microtubules. *Science.* 300:798–801.

Nakamura, Y., F. Tanaka, N. Haraguchi, K. Mimori, T. Matsumoto, H. Inoue, K. Yanaga, and M. Mori. 2007. Clinicopathological and biological significance of mitotic centromere-associated kinesin overexpression in human gastric cancer. *Br. J. Cancer.* 97:543–549.

Nitta, R., M. Kikkawa, Y. Okada, and N. Hirokawa. 2004. KIF1A alternately uses two loops to bind microtubules. *Science.* 305:678–683.

Ogawa, T., R. Nitta, Y. Okada, and N. Hirokawa. 2004. A common mechanism for microtubule destabilizers-M type kinesins stabilize curling of the protofilament using the class-specific neck and loops. *Cell.* 116:591–602.

Ovechkina, Y., M. Wagenbach, and L. Wordeman. 2002. K-loop insertion restores microtubule depolymerizing activity of a "neckless" MCAK mutant. *J. Cell Biol.* 159:557–562.

Rice, S., A.W. Lin, D. Safer, C.L. Hart, N. Naber, B.O. Carragher, S.M. Cain, E. Pechatnikova, E.M. Wilson-Kubalek, M. Whittaker, et al. 1999. A structural change in the kinesin motor protein that drives motility. *Nature.* 402:778–784.

Sablin, E.P., F.J. Kull, R. Cooke, R.D. Vale, and R.J. Fletterick. 1996. Crystal structure of the motor domain of the kinesin-related motor ncd. *Nature.* 380:555–559.

Sasaki, N., T. Shimada, and K. Sutoh. 1998. Mutational analysis of the switch II loop of *Dictyostelium myosin* II. *J. Biol. Chem.* 273:20334–20340.

Schief, W.R., R.H. Clark, A.H. Crevenna, and J. Howard. 2004. Inhibition of kinesin motility by ADP and phosphate supports a hand-over-hand mechanism. *Proc. Natl. Acad. Sci. USA.* 101:1183–1188.

Shimo, A., C. Tanikawa, T. Nishidate, M.L. Lin, K. Matsuda, J.H. Park, T. Ueki, T. Ohta, K. Hirata, M. Fukuda, et al. 2008. Involvement of kinesin family member 2C/mitotic centromere-associated kinesin overexpression in mammary carcinogenesis. *Cancer Sci.* 99:62–70.

Shipley, K., M. Hekmat-Nejad, J. Turner, C. Moores, R. Anderson, R. Milligan, R. Sakowicz, and R. Fletterick. 2004. Structure of a kinesin microtubule depolymerization machine. *EMBO J.* 23:1422–1432.

Suzuki, Y., T. Yasunaga, R. Ohkura, T. Wakabayashi, and K. Sutoh. 1998. Swing of the lever arm of a myosin motor at the isomerization and phosphate-release steps. *Nature.* 396:380–383.

Tomishige, M., N. Stuurman, and R.D. Vale. 2006. Single-molecule observations of neck linker conformational changes in the kinesin motor protein. *Nat. Struct. Mol. Biol.* 13:887–894.

Woehlke, G., A.K. Ruby, C.L. Hart, B. Ly, N. Hom-Booher, and R.D. Vale. 1997. Microtubule interaction site of the kinesin motor. *Cell.* 90:207–216.